Knowledge E
Engaging minds

Conference Paper

Influence of Solvent Additive 1,8-Octanedithiol on P3HT:PCBM Solar Cells

W. J. Wang[1], L. Song[2], X. H. Ren[1], H. Q. Fan[1], J. F. Moulin[3], and P. Müller-Buschbaum[2]

[1]State Key Laboratory of Solidification Processing, School of Materials Science and Engineering, Northwestern Polytechnical University, Xi'an 710072, China
[2]Technical University of Munich, Physics Department, Chair of Functional Materials, 85748 Garching, Germany
[3]Helmholtz Zentrum Geesthacht, Outstation at MLZ, 85747 Garching, Germany

Corresponding Author:
W. J. Wang
weijia.wang@nwpu.edu.cn

Selection and Peer-review under the responsibility of the ASRTU Conference Committee.

🔓 **OPEN ACCESS**

Abstract

A facile and efficient route is developed to improve the power conversion efficiency of poly(3-hexylthiophene-2,5-diyl):[6, 6]-phenyl-C61 butyric acid methyl ester (P3HT:PCBM) solar cells by processing solvent additive 1,8-octanedithiol (ODT) in the bulk heterojunction systems. The influence of ODT on polymer surface and inner morphology, crystallinity, and quantitative molecular miscibility of P3HT and PCBM is studied. The results show that ODT enhances the phase separation of P3HT and PCBM and the P3HT crystallinity, increases the solubility of PCBM in P3HT, and reduces the size of amorphous P3HT domains. A high concentration of ODT induces the formation of a PCBM enrichment surface layer, which is beneficial for the device performance.

Keywords: P3HT:PCBM, ODT, TOF-GISANS, morphology, miscibility

1. Introduction

1,8-octanedithiol (ODT) and 1,8-diiodooctane (DIO) as solvent additives are well known to tune the morphology of the active layer of organic solar cells, which typically leads to a significantly improved power conversion efficiency (PCE) of the processed solar cells [1–4]. For example, Chen et al. [2] demonstrated that interpenetrating P3HT:PCBM networks induced by 3 vol% ODT gave rise to the PCE enhancement of poly(3-hexylthiophene-2,5-diyl):[6, 6]-phenyl-C61 butyric acid methyl ester (P3HT:PCBM) solar cells. Razzell-Hollis et al. [3] found that an ODT concentration of 3 vol% significantly improved the P3HT molecular ordering. Cho et al. [4] showed that fibrilla structures of P3HT were formed with the aid of ODT, which led to an improved mobility of positive charge carriers. The structure characterization in these studies was mainly achieved with atomic force microscopy (AFM) measurements, which only gave information about surface morphology on a local scale. With respect to

How to cite this article: W. J. Wang, L. Song, X. H. Ren, H. Q. Fan, J. F. Moulin, and P. Müller-Buschbaum, (2018), "Influence of Solvent Additive 1,8-Octanedithiol on P3HT:PCBM Solar Cells" in *Sino-Russian ASRTU Conference Alternative Energy: Materials, Technologies, and Devices,* KnE Materials Science, pages 56–65. DOI 10.18502/kms.v4i2.3038

Page 56

organic solar cells, the charge carrier dissociation only occurs at the donor-acceptor interface, thus the inner morphology of the active layer dominates the charge carrier generation. Therefore, the understanding of the solvent additive on inner morphology of the active layer is highly demanded. Schaffer et al. utilized grazing incidence small-angle X-ray scattering (GISAXS) measurements to observe the increased domains sizes inside poly[2,6-(4,4-bis(2-ethylhexyl)-4H-cyclopenta[2,1-b;3,4-b']dithiophene)-alt-4,7(2,1,3-benzothiadiazole)]:[6, 6]-phenyl C71-butyric acid methyl ester (PCPDTBT: PC71BM) bulk heterojunction (BHJ) films by ODT processing, which was linked to the enhanced photovoltaic performance [5].

Time of flight grazing incidence small angle neutron scattering (TOF-GISANS) measurement is a powerful tool to probe the film structures. This advanced technique contains many different neutron wavelengths, which can be considered as a set of GISANS measurements [6]. By choosing a proper incident angle, the measurements allow characterizing the surface and inner film structures simultaneously. Moreover, TOF-GISANS measurements are able to precisely determine scattering length density (SLD) of the probed materials, which allows for a quantitative study of the molecular miscibility of donor and acceptor materials. In the present work, TOF-GISANS measurements are used to determine the morphology of P3HT:PCBM BHJ films treated with different volume concentrations of ODT. For a comparison, the surface morphology is characterized with AFM measurements as well. Moreover, the impact of ODT on P3HT crystallization is studied with razing incidence wide-angle X-ray scattering (GIWAXS) measurements. To link the experimental findings with the device performance, organic solar cells are fabricated out of the investigated P3HT:PCBM BHJ films to give a proof of practicability.

2. Methods

P3HT:PCBM BHJ films with different volume concentrations of ODT are prepared via a solution-based method. Firstly, ODT is dissolved in toluene with different volume concentrations (0, 1, 3, 5, 7, and 9 vol%) and then a weighed PCBM is added to individual ODT solution. Afterward, the solutions are put into a sand bath (55°C) for a complete dissolution of the solutes. Subsequently, the weighed P3HT powder is individually added to the PCBM solutions. After a complete mixing, the ready-to-use solution contains a total concentration of P3HT and PCBM of 18 mg mL^{-1} and a weight ratio of 1:0.8. For AFM, GIWAXS and TOF-GISANS measurements, all investigated films were deposited on silicon substrates via spin coating. For solar

cell devices, indium tin oxide (ITO)-coated glass sheets are etched with zinc powder and HCl to obtain the desired pattern. Afterward, the patterned ITO sheets are cleaned in sequence with Alconox solution, ethanol, acetone, and isopropanol in an ultrasonic bath and followed by oxygen plasma for 10 min. Separately, poly(3,4-ethylenedioxythiophene):poly(styrenesulfonate) (PEDOT:PSS) solution is ultrasonicated for 15 min and then filtered with a polyvinylidene fluoride (PVDF) filter (a pore size of 0.45 µm). Subsequently, the PEDOT:PSS solution is spin coated on the cleaned ITO substrates (3000 rpm, 60 s) and followed by an annealing process (150°C for 10 min). After being cooled down to room temperature, P3HT:PCBM BHJ films with different volume concentrations of ODT are spin coated on top. To complete organic solar cells, aluminum electrodes are thermally evaporated on top of the active layer under vacuum conditions. Finally, the obtained solar cells are thermally annealed (120°C for 10 min) in a N_2 filled glove box.

AFM measurements are performed by a JSPM-5200 scanning probe microscope (JEOL Ltd.) in noncontact (NF)-AFM mode. The GIWAXS measurements are carried out at an in-house instrument GANESHA 300 XLSAXS SYSTEM by JJ X-Ray System Aps. [7, 8]. The X-ray wavelength is 0.154 nm, a grazing incident angle is chosen as 0.2°, and a sample-to-detector distance is set to 106 mm. TOF-GISANS measurements are performed at the beamline REFSANS of the Helmholtz Zentrum Geesthacht at the neutron research source Heinz Maier-Leibnitz (FRM II), Garching, Germany. The wavelength band ranges from 0.20 to 1.48 nm. A grazing incident angle of 0.46° and a sample-to-detector distance of 10.52 m are selected for the experiments, respectively. The acquisition time is 18 h for each sample.

3. Results

AFM measurements are used to determine the influence of ODT on the surface morphology of P3HT:PCBM BHJ films. The obtained nanoscale topographies are depicted in Figure 1. The P3HT:PCBM BHJ film without ODT processing is denoted as the reference film. Figure 1a reveals that a uniform surface structure containing fine grains is present in the reference film. However, with increasing ODT concentrations, inhomogeneous films with large grains are observed, indicating a large scale phase separation occurs with the addition of ODT. In more detail, isolated island-like structures are present in the films with ODT of 3 and 5 vol%, as shown in Figures 1(c) and (d). Moreover, the grains are larger in the film with 5 vol% ODT than in the one with 3 vol% ODT. With a further increasing ODT concentration to 7 vol%, elongated worm-shaped domains

are observed at the sample surface rather than island-like structures (Figure 1(e)), suggesting a higher degree of the large scale phase separation of P3HT and PCBM. When the ODT volume concentration increases to 7 vol%, a layer of fine grains is present, which is correlated to a PCBM enrichment layer. A similar observation was reported by Schaffer et al., who demonstrated that a PCBM enrichment layer was formed at top of the active layer with the ODT treatment [5]. However, bicontinuous worm-shaped structures can still be seen underneath the thin PCBM enrichment layer, showing a similar feature as the film with 7 vol% ODT.
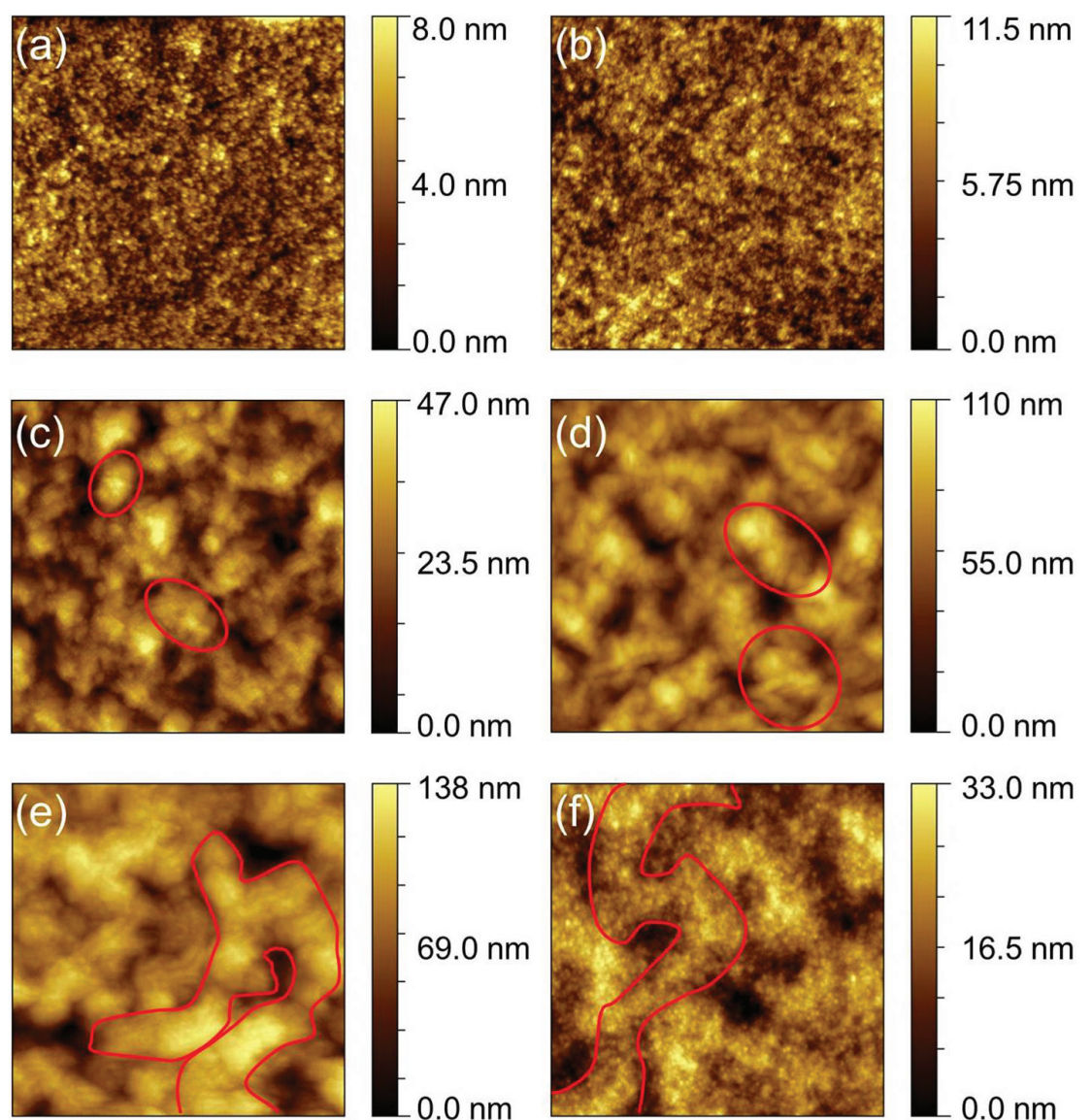

Figure 1: AFM topographic data (4×4 μm^2) of the P3HT:PCBM films with different volume concentrations of ODT: (a) 0 vol%, (b) 1 vol%, (c) 3 vol%, (d) 5 vol%, (e) 7 vol%, and (f) 9 vol%. The exemplary large structures are indicated by red lines in (c), (d), (e), and (f), respectively.

From the data analysis, the surface roughness of all films is extracted, reading 1 nm (0 vol%), 2 nm (1 vol%), 8 nm (3 vol%), 19 nm (5 vol%), 23 nm (7 vol%), and

6 nm (9 vol%), respectively. The film roughness increases with increasing amount of ODT up to 7 vol%, but decreases with a further increase of ODT to 9 vol%. Therefore, we conclude that a higher degree of the phase separation and an enhancement of ordered structures occur with the addition of ODT, which was frequently observed for organic active layers after thermal and/or solvent annealing [9, 10]. In general, the enhanced phase separation induced by ODT is ascribed to the different solubility of P3HT and PCBM in ODT. The difference facilitates a significant demixing between P3HT and PCBM. However, when the amount of solvent additive reaches a threshold, finer structures tend to form at the sample instead of large phase separation. The occurrence is due to a suppression of demixing by an earlier aggregation of P3HT.

To probe the inner morphology difference of P3HT:PCBM BHJ films processed with different amount of ODT, GISANS measurements are performed. The representative 2D GISANS data with a selection of neutron wavelengths for the reference film are displayed in Figure 2. It can be seen that the overall scattering intensity varies with wavelengths, which is due to the fact that the distribution of the incoming neutron flux differs as a function of the wavelength. Moreover, the position of Yoneda peaks shifts upward with increasing neutron wavelength, which is ascribed to the critical angle of the probed materials being proportional to the wavelength. In order to illustrate the features along the surface normal, vertical line cuts are performed on 2D GISANS data at q_y = 0. From quantitative analysis of Yoneda peak position, the SLDs of P3HT, PCBM, and silicon are obtained, which agrees well with the theoretical values. Moreover, the SLD of molecularly mixed phase of P3HT:PCBM is determined for each film.
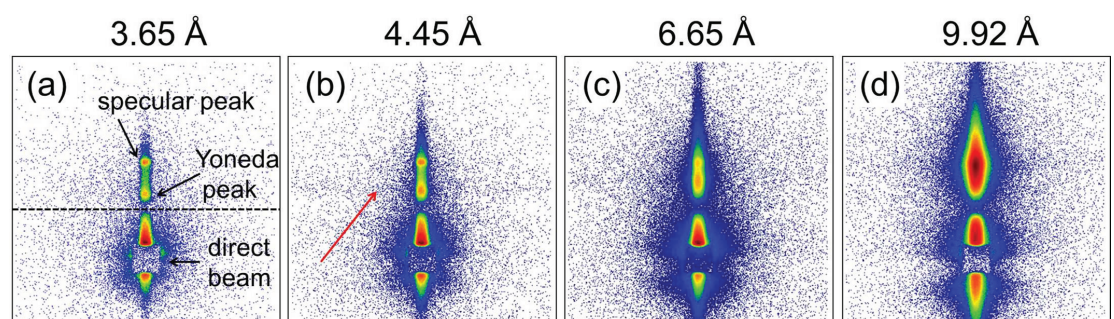

Figure 2: Exemplary presentations of 2D GISANS data of the reference film.

Then the formula $SLD_{P3HT} + \gamma_{PCBM} SLD_{PCBM} = SLD_{P3HT:PCBM}$ is used to determine the fraction of molecularly dispersed PCBM (γ_{PCBM}) in P3HT matrices. The obtained results are shown in Figure 3. It is noticeable that the γ_{PCBM} is about 12.5% in the reference film, which is smaller than the value reported in the P3HT:PCBM BHJ system prepared from chlorobenzene. The difference in γ_{PCBM} implies that the host solvent has an impact on the molecular miscibility of P3HT and PCBM. With the addition of ODT,

an increase of γ_{PCBM} is observed. Owing to a relatively lower solubility of P3HT in ODT, P3HT is easier to be expelled from the mixture of P3HT and PCBM. As a result, more PCBM remains in the molecularly mixed P3HT:PCBM phase. However, with increasing ODT content, γ_{PCBM} stays almost stable. This occurrence might be due to a saturation of the solubility of PCBM in P3HT matrices. The horizontal line cuts are taken at the position of the PCBM Yoneda peak to obtain information about film lateral structures. From data modeling, the extracted domain sizes and center-to-center distances are displayed in Figure 4 as a function of ODT content. For small-sized structures, the size remains constant irrespective of ODT content, whereas a continuous decrease of the center-to-center distance is observed with increasing amount of ODT. For large-sized structures, the center-to-center distance has a similar trend with the small-sized counterparts, whereas the domain size increases gradually with increasing ODT content. The information of both small-sized and large-sized structures implies a decrease of P3HT domain sizes with increasing ODT concentration. As a consequence, an enhancement of charge generation in the corresponding active layers is expected.
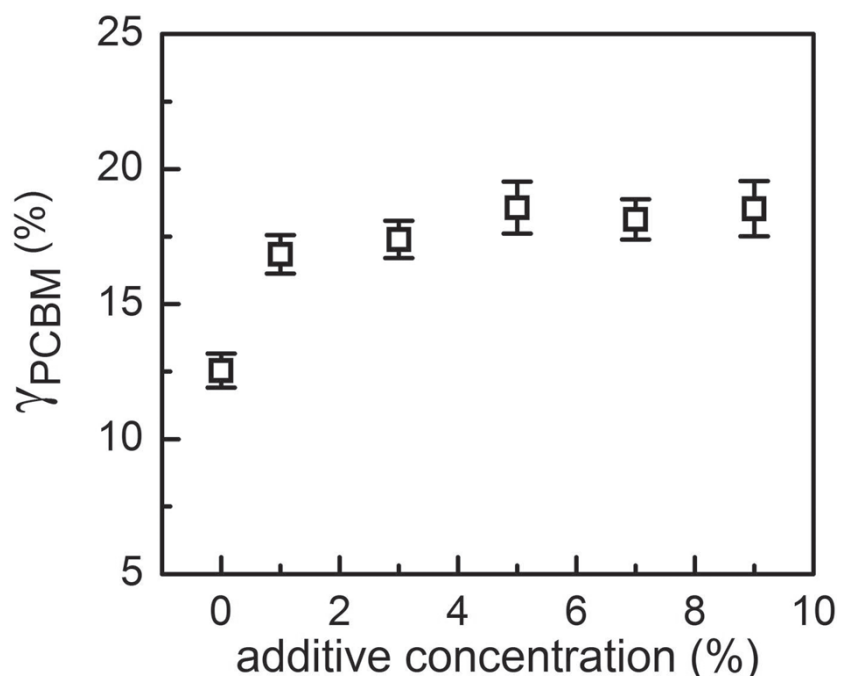

Figure 3: The fraction of molecularly dispersed PCBM (γ_{PCBM}) in P3HT matrices as a function of ODT content.

GIWAXS measurements are carried out to investigate the crystalline order in the P3HT:PCBM BHJ system. The horizontal and vertical integrals of 2D GIWAXS data of the films are depicted in Figure 5. It can be seen that the P3HT (100) peak is more pronounced in the horizontal direction than in the vertical direction for the reference film, indicating a preferred face-on orientation of P3HT (100) crystal planes. With increasing
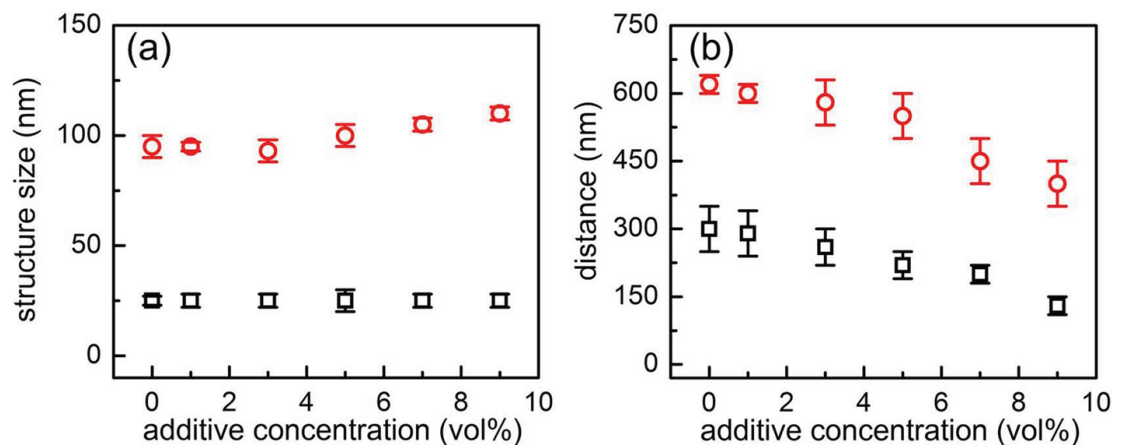
Figure 4: The extracted (a) structure size and (b) center-to-center distance of the P3HT:PCBM films with various ODT concentration. Hollow squares indicate the small-sized structure, and hollow circles indicate the large-sized structure.

ODT concentration, the (100) peak are more pronounced in the vertical integral versus the horizontal integral, suggesting a preferred edge-on orientation induced by ODT. However, a decrease of the (100) peak is observed for the film with 9 vol% ODT, meaning that excessive ODT lowers the P3HT crystallinity. Moreover, the (100) lattice constants are determined to be 1.7-1.8 nm for both horizontal and vertical directions from the position of the (100) peak, which are in line with the values reported in literature [11, 12]. From the analysis of the horizontal integrals, the P3HT crystals with a face-on orientation decrease from a size of (8.6 ± 0.2) nm to (7.2 ± 0.2) nm with increasing ODT concentration to 7 vol%. While with further increase of ODT content to 9 vol%, crystal size increases to (9.7 ± 0.3) nm. In contrast, the edge-on P3HT crystal shows an opposite tend with the face-on counterparts. The size firstly increases from (6.6 ± 0.1) nm to (8.3 ± 0.2) nm and then decreases to (7.2 ± 0.3) nm.

Figure 6(a) shows the *J-V* characteristics of P3HT:PCBM BHJ solar cells with various ODT content. The extracted values of PCE and short-circuit current density (J_{sc}) are displayed in Figures 6(b) and (c). It can be seen that both PCE and J_{sc} are improved with increasing volume concentration of ODT. For J_{sc}, the improvement with increasing ODT amount is mainly contributed to an optimized inner morphology of the P3HT:PCBM active layer and a higher crystallinity of P3HT. With increasing ODT content to 7 vol%, the decreased size of P3HT domains and increased amounts of P3HT crystals result in a gradual increase of J_{sc}. For the film with 9 vol% ODT, although the P3HT crystallinity decreases, the formation of a PCBM enrichment layer on top of the active layer acts as a hole-blocking layer, which is beneficial for charge carrier collection and thereby leads to an enhanced J_{sc}. For PCE, the improvement mainly originates from the enhancement of J_{sc} as they show a similar growth rate trends. Therefore, we conclude that ODT
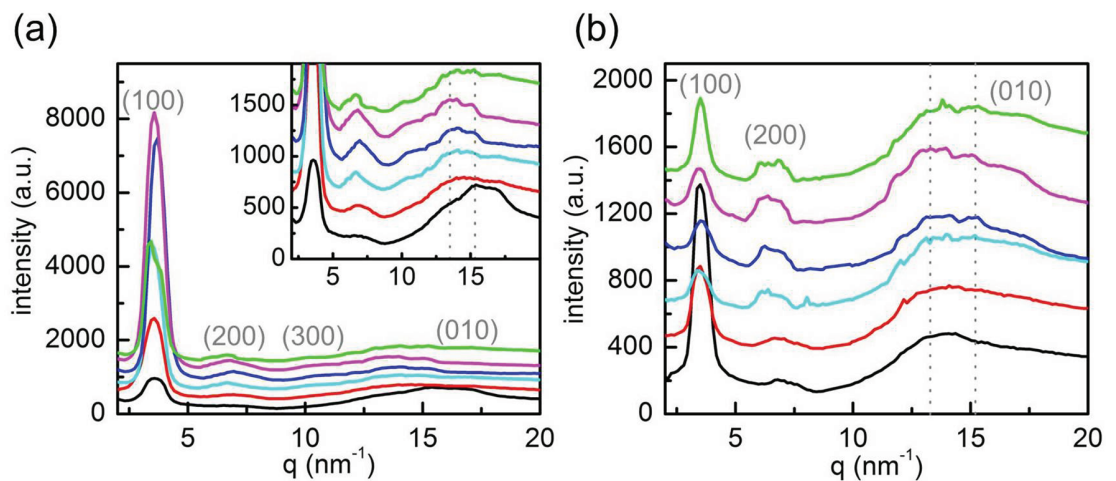
Figure 5: (a) The (a) vertical and (b) horizontal sector integrals of the P3HT:PCBM films with various ODT concentration (0 vol%, 1 vol%, 3 vol%, 5 vol%, 7 vol%, and 9 vol% from bottom to top). In the inset of panel (a), zoom into the q range above 5 nm^{-1}.

processing optimizes the architecture of the active layer regarding the domain size, the polymer crystallinity and the formation of enrichment layers, which leads to an improved device performance.
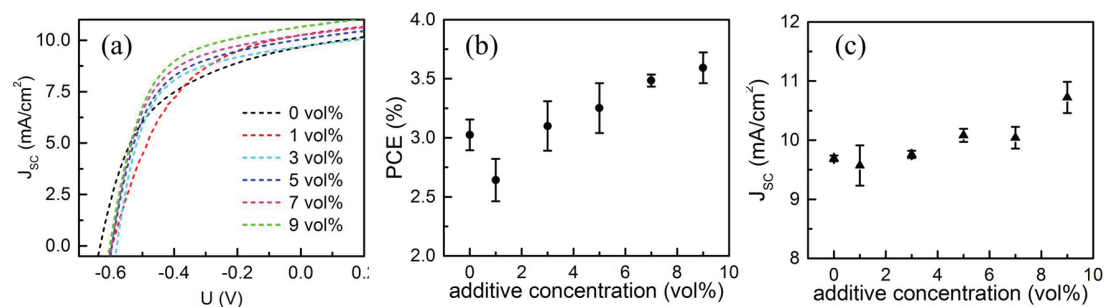

Figure 6: (a) J-V characteristics of P3HT:PCBM BHJ solar cells with various ODT concentration. The extracted (b) PCE and (c) J_{sc} as a function of ODT content.

4. Conclusion

In summary, the influence of the solvent additive ODT on P3HT:PCBM BHJ systems is investigated from morphological perspective. The AFM measurements verify a higher degree of phase separation of P3HT and PCBM. TOF-GISANS measurements observe a decreased P3HT domain size and an increased fraction of the molecularly dispersed PCBM, which is good for charge carrier dissociation. Moreover, it is found that a PCBM enrichment layer resides on top of the active layer. GIWAXS measurements give a proof that P3HT crystallinity increases with increasing ODT content, which is beneficial for hole transport. To link these findings with photovoltaic performance, P3HT:PCBM BHJ

solar cells various ODT content are produced. The PCE and J_{sc} improve with increasing ODT concentration, which is caused by the decreased P3HT domain size, increased polymer crystallinity and the formation of enrichment layers.

Acknowledgements

References

[1] Gholamkhass, B., Peckham, T. J., and Holdcroft, S. (2010). Poly(3-hexylthiophene) bearing pendant fullerenes: Aggregation vs. self-organization. *Polymer Chemistry*, vol. 1, pp. 708–719.

[2] Chen, H. Y., Yang, H., Yang, G., et al. (2009). Fast-grown interpenetrating network in poly(3-hexylthiophene): Methanofullerenes solar cells processed with additive. *Journal of Physical Chemistry C*, vol. 113, pp. 7946–7953.

[3] Razzell-Hollis, J., Tsoi, W. C., and Kim, J. S. (2013). Directly probing the molecular order of conjugated polymer in OPV blends induced by different film thicknesses, substrates and additives. *Journal of Materials Chemistry C*, vol. 1, pp. 6235–6243.

[4] Cho, S., Nho, S. H., Eo, M., et al. (2014). Effects of processing additive on bipolarfield-effect transistors based on blends of poly(3-hexylthiophene) and fullerene bearing long alkyl tails. *Organic Electronics*, vol. 15, pp. 1002–1011.

[5] Schaffer, C. J., Schlipf, J., Indari, E. D., et al. (2015). Effect of blend composition and additives on the morphology of PCPDTBT:PC71BM thin films for organic photovoltaics. *ACS Applied Materials & Interfaces*, vol. 7, pp. 21347–21355.

[6] Müller-Buschbaum, P., Kaune, G., Haese-Seiller, M., et al. (2014). Morphology determination of defect-rich diblock copolymer films with time-of-flight grazing-incidence small-angle neutron scattering. *Journal of Applied Crystallography*, vol. 47, pp. 1228–1237.

[7] Kampmann, R., Haese-Seiller, M., Kudryashov, V., et al. (2004). The potential of the horizontal reflectometer REFSANS/FRM-II for measuring low reflectivity and diffuse surface scattering. *Physica B*, vol. 350, pp. E763–E766.

[8] Kampmann, R., Haese-Seiller, M., Kudryashov, V., et al. (2006). Horizontal ToF-neutron reflectometer REFSANS at FRM-II Munich/Germany: First tests and status. *Physica B*, vol. 385–386, pp. 1161–1163.

[9] Yao, Y., Hou, J., Xu, Z., et al. (2008). Effects of solvent mixtures on the nanoscale phase separation in polymer solar cells. *Advanced Functional Materials*, vol. 18, pp. 1783–1789.

[10] Li, G., Shrotriya, V., Huang, J., et al. (2005). High-efficiency solution processable polymer photovoltaic cells by self-organization of polymer blends. *Nature Materials*, vol. 4, pp. 864–868.

[11] González, D. M., Körstgens, V., Yao, Y., et al. (2016). Improved power conversion efficiency of p3Ht: PCBM organic solar cells by strong spin-orbit coupling-induced delayed fluorescence. *Advanced Energy Materials*, vol. 5, p. 1401770.

[12] Ruderer, M. A. (2012). Morphology of polymer-based films for organic photovoltaics. PhD thesis, Technische Universitat Munchen, Munich, Germany.